Investigations into the Effects of 3-Dimensional Geometric Parameters on the Structural Design of an Adaptive Morphing Wingtip

André Ferreira Tribolet de Abreu
andre.abreu@ist.utl.pt

Instituto Superior Técnico, Lisboa, Portugal

October 2014

Abstract

As part of the EU FP7 project NOVEMOR, a droop-nose adaptive morphing wingtip (AMWT) is being designed at the DLR (German Aerospace Center), with the potential to reduce drag and substitute classical wing control surfaces. It is composed by a fiberglass composite material skin with an optimized thickness distribution and a double-L stringer whose position is also optimized. The AMWT is activated via a compliant mechanism, connected at the stringer, and the traditional tools used for its design do not take into account the 3D geometric parameters present in a wingtip such as tapering and sweep angle.

The present thesis proposes a methodology to investigate how the 3D geometric parameters affect the output of the compliant mechanism and the shape morphing of the wingtip. Furthermore the methodology is applied to a modeled wingtip similar to the one being used in project NOVEMOR in order to aid and provide data for its design process. The 3D parameters considered in this thesis are sweep angle, tapering in the chord direction and tapering in the thickness direction.

The analysis is divided into two parts: a first analysis focused on the effects of the 3D geometrical parameters on the morphing shape of the wingtip comparing it to a defined ideal scenario; a second analysis focused on the effects on the morphing mechanism.
Keywords: compliant mechanism, droop-nose, morphing wingtip, topology optimization

1. Introduction

In the aeronautical industry, the term morphing is used when referring to 'a set of technologies that increase a vehicle's performance by manipulating certain characteristics to better match the vehicle state to the environment and task at hand' [14]. The exact type or extent of the geometrical changes necessary to qualify a structure for the title of 'shape morphing' has no consensus between researchers in the area since the above definition can also include established technologies such as flaps, slats, ailerons or retractable landing gear while the term morphing contains a connotation of 'radical shape changes or shape changes only possible with near-term or futuristic technologies' [3].

Given the review made in [3], wing morphing concepts can be classified into three major groups according to which wing parameter is affected as illustrated in Fig.1: planform alteration (changes in sweep, span or chord), out-of-plane transformation (twist, dihedral/gull and spanwise bending) and airfoil alterations (camber and thickness).

In this thesis, the shape morphing being analyzed lies in the 'airfoil alteration' category where the curvature of the leading edge has a clean (for cruise) and a droop (for take-off and landing) configuration.

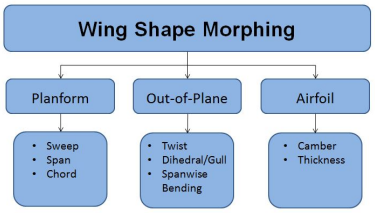

Figure 1: Classification of shape morphing wing concepts according to [3]

The great advantage of the use of shape morphing wings is the potential to radically expand an aircraft's flight envelope. A morphing aircraft will be more competitive compared to conventional aircrafts as more mission tasks are added to their requirements [3]. In order to be able to fly at a range of flight conditions, wings are designed in or-

der to satisfy several different (many times opposing) requirements thus often leading to sub-optimal performance at each flight condition [3]. An ideal example of a morphing wing is a wing capable of continuously adjusting its airfoil shape increasing its lift/drag ratio for each different flight condition [12].

Several challenges occur with the use of morphing technologies, most of them rely on the existence of a flexible skin with conflicting requirements: it has to be sufficiently soft to allow shape changes but at the same time stiff enough to maintain the desired shape under aerodynamic loads. Also, the strictness of these requirements change for different flight conditions [3].

The use of a compliant mechanism to achieve morphing is one of the key features of the AMWT, bringing the potential associated advantages such as weight savings, reduced part and assembly costs, and the elimination of backlash [13].

A compliant mechanism, as defined in [8], is a single-piece flexible structure that delivers the desired motion by undergoing elastic deformation (as opposed to using movable joints) that can be designed to obtain any desired input/output force/displacement characteristics. Traditional mechanisms are designed to be strong and stiff and are usually assembled from discrete components [8]. A compliant mechanism is designed to be flexible enough to transmit the desired motion and at the same time to be stiff enough to withstand the external loads [9].

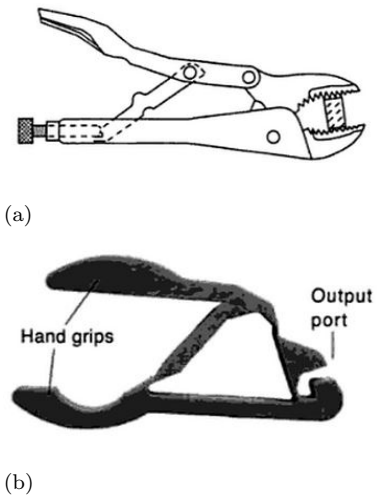

(a)

(b)

Figure 2: Examples of (a) rigid body and (b) compliant crimping mechanisms [6]

Several methods exist for the design of compliant mechanisms and most of them can be divided into methods based on the pseudo-rigid body model or based on optimization [1].

Optimization based design methods view flexible mechanisms as flexible continua and are used to design mechanisms with distributed compliance where large portions of the structure deform when it's loaded [1].

Topology optimization is the most general level of structural optimization of a continuum mechanism [6] (followed by shape and size optimization) where given a design domain, the algorithms created consider all possible ways of distributing the material in the domain in order to obtain the desired output [1].

1.1. AMWT Design Process

The 3D geometry of the wingtip is given by Embraer and as can be seen from Fig.3, it can be characterized by a sweep angle and tapering in chord and thickness directions. The presence of these parameters result in a complex morphing design and manufacture processes.

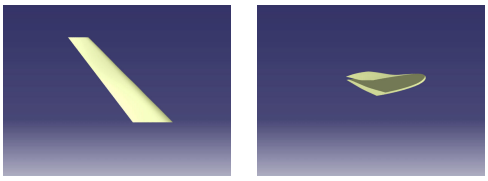

(a) (b)

Figure 3: 3D geometry of the Embraer wingtip

The design process of the AMWT is currently being developed at the DLR by Dr. Srinivas Vasista and the following description is based on the paper that is being written on the topic [13] regarding the construction of a demonstrator model for the droop-nose morphing device. The leading edge of the AMWT must be able to assume two different shapes: the clean target shape without actuation input and the droop target shape when actuated.

The structural design of the AMWT goes through three stages: design of the wingtip skin; design of the compliant mechanism and finally the design of the support for the compliant mechanism.

For the skin design stage, the DLR design tool [7] is used and data regarding the design domain geometry, location of the connection points, target displacements and output forces to be delivered by the mechanism, and the stiffness of the skin are obtained. This data is then used as input for the second stage where the compliant mechanism is designed via topology optimization using the solid isotropic material with penalisation (SIMP) material model [4]. Data obtained from this stage is then transfered to the design of the support, namely design domain geometry, material and thickness (as the design is monolithic), reaction forces from the compliant mechanism and the actuator and their

locations. With this data the support is designed, again using topology optimization.

2. Methodologies Chosen

As stated before, two analysis were made. The first, regarding the effects on the shape morphing of the wingtip, will be denoted as SMA (shape morphing analysis) and the second, regarding the effects on the compliant mechanism, will be denoted as CMA (compliant mechanism analysis).

2.1. Analysis Concept

As a first step, a parameterized CAD model of the geometry of the wingtip is constructed where it is possible to change parameters such as sweep angle and taper ratio. The next step is to apply a loading case to various wingtips with different 3D geometrical parameters, simulating the actuation of the morphing mechanism (this is done using finite element analysis software). Finally the obtained morphing shape is compared to an ideal case to determine the differences in shape.

The first problems that arose were how to define an ideal morphing shape for a certain profile of the considered 3D wingtip and how to obtain results comparable between different wingtips. To solve these problems, it is assumed that each wingtip will contain two morphing mechanisms, one located at 1/4 of the span (Profile 4 or P4) and the other located at 3/4 of the span (profile 2 or P2). The 3D geometrical parameters that were considered are sweep angle, tapering in the chord direction and tapering in the thickness direction.

Now it is necessary to define the ideal morphing shape of the considered profiles. This was done by building uniform wingtips (no sweep angle nor tapering) with a cross-section identical to the profile where the displacement is being applied in the non-uniform wingtip. So, for example, when considering a wingtip with taper ratio of 0.8, it is necessary to consider a uniform wingtip scaled to 0.85 of the root profile (to match P2) and another one scaled to 0.95 of the root profile (to match P4). The same displacements are then applied to those uniform wingtips and the resulting morphing shape is what will be considered as ideal.

For CMA it was necessary to also build a parameterized CAD model of the compliant mechanism to incorporate with the different wingtips. In SMA, to simplify the analysis and be able to analyze a bigger variety of different wingtips, only the desired output of the mechanism is taken into account, substituting it by desired displacements located where the mechanism would be attached to the stringer. With this simplification it is possible to eliminate the step of designing the mechanisms for each different wingtip. The same displacements are applied on both sections of the wingtip (P2 and P4) assuming that for each different profile considered, a morphing mechanism could be designed to obtain those displacements.

In CMA, results regarding the shape morphing of the wingtip are also discussed in order to validate the above mentioned simplification made in SMA.

2.2. CAD Models

Wingtip

In order to test several different wingtips, a parameterized geometrical model was built, using CATIA software, based on the inboard profile of the wingtip given by Embraer. Since the aim of the NOVEMOR project is to design a droop-nose adaptive morphing wingtip, only the leading edge of the wingtip is modeled and so in future references, when using the term wingtip, it is meant the leading edge of the wingtip.

In Fig.4 are listed the six parameters that control the geometry of the wingtip. The first two change the scaling of the root profile allowing to model different uniform wingtips for the purpose of obtaining the ideal morphing shape. The third parameter defines the span and as said before is set at a fixed value of $1500mm$. The fourth parameter changes the sweep angle and finally, the last two parameters, control the tapering in the chord and thickness direction (relative to the dimensions of the inboard profile which are defined by the first two parameters).

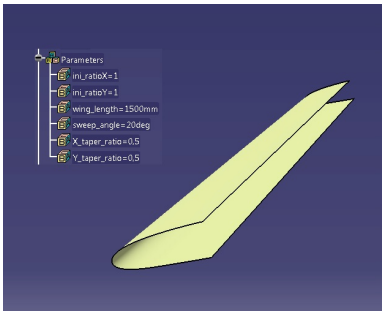

Figure 4: CAD model of a wingtip with 20°sweep angle and 0.4 taper ratio in both chord and thickness direction

The CAD model created allows to rapidly obtain different wingtip geometries for future morphing analysis.

Compliant Mechanism

The first task was to determine how to model the compliant mechanisms for the different wingtips that are considered. It is not feasible to go through the entire topology optimization process (which requires data regarding the geometry of the wingtip)

to obtain the adequate mechanism for each different profile and it is necessary to have flexibility in terms of the load cases that will be applied (topology optimization results in a compliant mechanism optimized for a specified displacement case) thus it was decided to use a compliant mechanism already modeled for a profile of the Embraer wingtip [13] and adapt it to fit the different wingtips that will be considered.

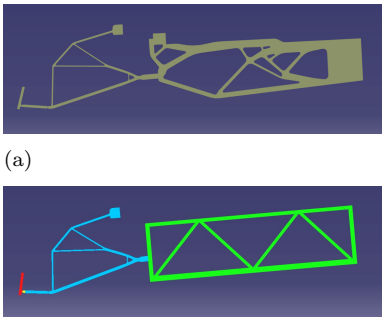

(a)

(b)

Figure 5: (a) Optimized Mechanism and (b) Adapted parameterized mechanism

The resulting mechanism is shown in Fig.5b. For short, the parameterized mechanism model created allows for scaling of the green section in both X and Y directions, scaling of the blue section in all directions at the same time, positioning of Point A and positioning of Point B in order to align the red section with the stringer of the wingtip it will be inserted in.

2.3. FE Models

The element type chosen was SHELL181 which is a four-node element with six degrees of freedom at each node (translation and rotation for x, y and z axes) being suitable for the thin shell structure that is the considered wingtip.

For the wingtip an isotropic material was chosen with an elastic moduli of $42GPa$ and a Poisson's ratio of 0.26. These values were chosen to simulate the actual fiberglass composite material that is being considered for the construction of the wingtip. Finally a uniform thickness of $2mm$ was chosen for the whole structure since it is close to the values obtained in the skin optimization that is being done.

For the mechanism the thickness was set to $5mm$. An isotropic material was used with an elastic moduli of $70GPa$ and a 0.35 Poisson's ratio in order to simulate the material properties of Aluminum 7075, which is the material being considered for the construction of the mechanism.

As boundary conditions, the nodes on the edges of the wingtip and all nodes in the trailing edge of the mechanism that mark the end of the leading edge were fixed in all six degrees of freedom *i.e.* no translation nor rotation. Furthermore, the node where the actuator would apply the force in the mechanism, only has only two degrees of freedom: translation along the x axis and rotation around the z axis simulating the presence of a linear actuator connected to the mechanism.

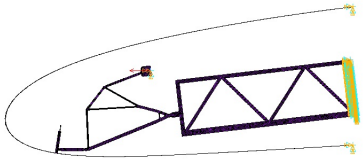

Figure 6: Wingtip and Mechanism boundary conditions

To simulate the actuation of the morphing mechanism for SMA, as said before, displacements are applied to the stringer at 1/4 and 3/4 of the span. It was decided to apply these displacements on the first bottom node of the stringer.

2.4. Load Cases

In order to obtain comparable results in SMA, the applied displacements are equal for P2 and P4 and for all the different wingtips. The selected values for displacement were 10mm in the negative y axis direction and 1mm in the positive x axis direction.

During the discussion of the results in SMA it was found that another load case should also be considered, LC0, where the magnitude of the displacements applied were scaled, from the above mentioned values, according to the tapering of the wing.

Relative to CMA, two load cases were considered. The first, LC1, is to apply displacements with the same magnitude and location as in SMA (LC0) in order to compare results in terms of ideal and actual morphing shape of the wingtip skin with and without the mechanism. The second, LC2, is to apply a force in the x direction where the actuator would be connected, in order to better simulate the actual behavior of the compliant mechanism when inserted in a wingtip with 3D geometrical parameters.

Profile X-scaling	**Profile Y-scaling**	**SR+SB** $[mm^2]$	**Applied force** $[N]$
1.0	1.0	1675.86	201
0.625	1.0	654.63	79
0.875	1.0	1283.08	154
1.0	0.625	654.63	79
1.0	0.875	1283.08	154
0.625	0.625	654.63	79
0.875	0.875	1283.08	154
Force-to-area ratio $[N/mm^2]$		0.12	

Table 1: Magnitude of applied forces for each specific type of Profile (LC2)

For LC2 it is necessary to define a constant parameter. The ratio between applied force and mechanism area (the area of SG was not taken into account since it has only support purposes and will

not influence the load path significantly) was chosen as the most suitable control parameter since the mechanism area is the simplest measurable property of the different compliant mechanisms used for the different wingtips. The value of the force-to-area ratio was chosen as the largest at which the FE solutions of all the wingtips converge (1).

2.5. Result Analasys Tool

With all the data that is possible to obtain, it becomes necessary to create tools that can filter the relevant data for the purposes of this work. Four main MATLAB scripts were written (*'ansys_read.m'*, *'displ_wing_analysis.m'*, *'SSF_analysis.m'* and *'displ_error_analysis.m'*) that extract and analyze the relevant data.

$$e = \frac{u_i^I - u_i^A}{u_i^I}, \quad i = x, y \tag{1}$$

Fig.7 illustrates the concept being used to analyze the effects of 3D geometrical parameters. Of course it is not possible to quantify the effects visually so the script also calculates the node displacement errors, defined by Eq.1 for each node.

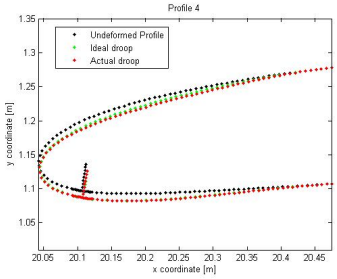

Figure 7: Ideal versus actual morphing shape of P4 of a wingtip with 0.5 X and Y taper ratio

3. SMA

In order to isolate the effects of the variation of each parameter individually, 3 sets of wingtips were created: a set of wingtips with different sweep angles ranging from 0° to 40° in steps of 5°; a set of wingtips with X-taper ratios ranging from 0.4 to 1.0 in steps of 0.1; and a set of wings with Y-taper ratios ranging from 0.4 to 1.0 in steps of 0.1.

Following is a discussion of the results obtained when the methodology developed was applied to the above mentioned sets of wingtips.

3.1. Results Discussion

In terms of the x and y components of the displacement errors, it is possible to infer that sweep angle affects the morphing shape at a much lower level than both types of tapering considered. Of course one cannot say that a step of 5° in sweep angle is a directly comparable geometrical parameter change to a 0.1 step in taper ratio but with a global view of the scope in which the parameters varied the comparison is possible. The percentile 90 for varying sweep angle has an almost linear behavior staying below 10% for both profiles and components of the displacement.

Now comparing the effects between X and Y-taper ratio, one can see how one affects more significantly a different profile than the other. From the percentile 90 data obtained it is clear that X-tapering has a greater affect on the inboard profile (P4) while Y-tapering has a greater affect on the outboard profile (P2).

It is important to keep in mind that X-tapering decreases the ratio between the horizontal and vertical dimensions of the profile along the span of the wingtip while Y-tapering increases this profile aspect ratio. So the fact that remains true for both types of tapering is that for the same wing, the profile which presents a bigger aspect ratio is going to display larger errors (larger values for the percentile 90).

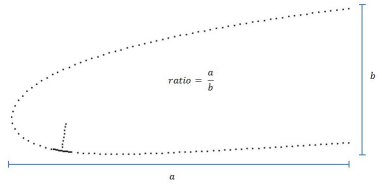

(a)

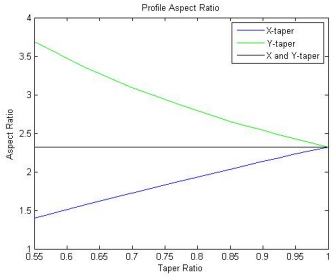

(b)

Figure 8: (a) Profile aspect ratio definition and (b) Relation between tapering and profile aspect ratio

Also, comparing both types of tapering, it can be concluded that in general, Y-tapering will result in larger errors than X-tapering. This can be due to the fact that a 0.1 X-taper ratio step does not result in an equal profile aspect ratio step then for the case of a 0.1 Y-taper ratio step. Fig.8b shows how aspect ratio behaves when tapering is introduced, it can be seen that the green curve has a slightly higher slope than the blue curve meaning that a variation of 0.1 Y-taper results in a bigger aspect ratio change than a 0.1 X-taper step. Still, this difference between slopes only results in around 5% difference between the aspect ratio percentual increase (or decrease) of

a 0.1 X and Y-taper step. Thus it does not seem to account for the larger errors shown in Y-tapering, reinforcing the conclusion stated at the beginning of this paragraph.

To remove the profile aspect ratio variable from the effects of tapering, Fig.9 shows the evolution of the percentile 90 of the displacement errors for the case when both types of taper ratios are varied at the same time in equal steps.

With the profile aspect ratio variable controlled, it can be seen that the inboard profile displays higher errors than the outboard profile. A possible explanation is the fact that for both profiles, the applied displacements have equal values even though the area bounded by the inboard profile is larger than the area bounded by the outboard profile. In other words, for the same displacement, the larger profile of a wingtip will display larger errors when tapering is present.

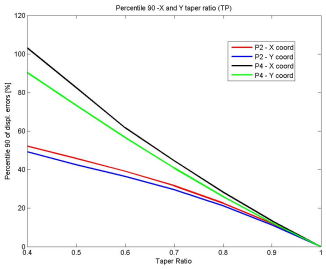

Figure 9: Percentile 90 for varying both types of taper ratios

To investigate the correlation between profile size and the magnitude of applied displacements, three tapered wings were analyzed applying LC0. The first wingtip has a X-taper ratio of 0.5, the second wingtip has a Y-taper ratio of 0.5 and the third wingtip has a X and Y-taper ratio of 0.5.

Table 2 displays the percentile 90 of the displacement errors for the above mentioned wingtips for the case of constant applied displacements while Table 3 displays the percentile 90 for the same wingtips but for the case where the applied displacements are scaled according to tapering.

Percentile 90 [%]						
X/Y taper	**0.5/1.0**		**1.0/0.5**		**0.5/0.5**	
Component	**x**	**y**	**x**	**y**	**x**	**y**
P2	4.42	3.24	128.46	133.06	45.81	42.51
P4	58.1	57.46	34.68	32.26	82.47	73.28

Table 2: Displacement error Percentile 90 for applied displacements of $1mm$ and $-10mm$ in the x and y directions respectively

Comparing both tables, it is noticeable how scaling the applied displacement in the X axis has so little affect on the resulting displacement errors having a maximum of 3% change between the percentile 90 values while in the case of scaling the applied displacements along the Y axis, the percentile 90 values drop to less than half. This indicates that the applied displacements in the Y axis are the main source of the morphing shape errors (which would be expected since the Y component of the displacement is one order of magnitude larger than the X component) and its value will be a decisive criteria when deciding if the 2D optimization will remain valid for the 3D wingtip.

Percentile 90 [%]						
X/Y taper	**0.5/1.0**		**1.0/0.5**		**0.5/0.5**	
Component	**x**	**y**	**x**	**y**	**x**	**y**
P2	4.51	3.14	53.23	52.74	2.58	2.40
P4	58.42	57.79	14.78	14.09	7.48	6.62

Table 3: Displacement error Percentile 90 for applied displacements scaled according to taper ratio values

Furthermore, Tables 2 and 3 show that scaling both components of the displacements reduces the displacement error percentile 90 to less than 1/10 of its original value. This reduction can be explained by the decrease in the value of the Y component of the applied displacement, but as seen before, it would only account for reducing the percentile 90 to around half of its original value. Another factor that can explain the rest of this reduction is the resulting droop angle of the wingtip. Having a large difference between the target droop in P2 and P4 may cause higher displacement errors.

Droop Angle [°]						
X/Y taper	**0.5/1.0**		**1.0/0.5**		**0.5/0.5**	
Displacement	**not scaled**	**scaled**	**not scaled**	**scaled**	**not scaled**	**scaled**
P2	1.622	1.621	1.025	0.6367	1.631	1.010
P4	1.153	1.152	1.011	0.882	1.157	1.008

Table 4: Droop angles of wingtips resulting from scaled and not scaled applied displacements

Cross checking Table 4 with Tables 2 and 3, it seems that the difference between P2 and P4's target droop angle is also correlated to displacement errors. In the case of a X-tapered wing, the droop angle difference between profiles doesn't significantly change when the X component of the applied displacement is scaled (also the Y component of the applied displacement remains constant) thus the percentile 90 of the displacement errors also does not change significantly. In the case of Y-tapering, the droop angle difference increases, when scaling the applied displacements, but the Y component of those displacements decrease with the scaling and so the percentile 90 of the errors decreases suggesting that the magnitude of the Y displacement has a higher influence on the morphing shape than the droop angle difference. Finally in the case

of X and Y-tapering both the Y component of the applied displacements and the droop angle difference decrease when the applied displacements are scaled thus resulting in a large displacement error percentile 90 drop.

To view the effect of having all three 3D geometrical parameters present in a wingtip, the sweep angle was varied for two different wingtips, one with 0.8 X and Y-taper ratio and another with 0.5 X and Y-taper ratio. Fig.10 shows that for tapered wings, the introduction of sweep angle can actually help decrease the percentile 90 of the displacement errors, specially for the outboard profile.

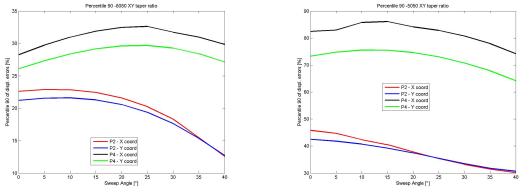

(a) (b)

Figure 10: Percentile 90 for varying sweep angles: (a) 0.8 taper ratio relative to both x and y axis and (b) 0.5 taper ratio relative to both x and y axis

Regarding the location of the errors in a profile, the data consistently shows that, for both types of tapering, errors start to grow significantly along the top section of the profile and in the bottom section (before the stringer) errors are usually low, under 10%. Meaning that the top section's morphing shape is the area in the profile most affected by tapering.

As for the z component of the displacement, there is a tendency for its value to increase with the increasing geometrical change resulting from varying parameters. Between the two types of tapering, Y-tapering results in displacements usually two times larger than X-tapering. It is noticeable that, in this case it is the sweep angle that increases the z displacement the most, displaying values of one order of magnitude higher than for the two cases of tapering. Still, the highest z displacement component has a value of $1.7mm$ which is very small when compared to the span of the wingtip ($1500mm$). In the end, the importance of how much displacement occurs in the z direction will depend on how much strain and stress will result in the morphing compliant mechanism.

4. CMA

In the previous chapter, the analysis made excludes the actual presence of the morphing mechanisms in the wingtip. Tapering and sweep angle will not only affect the resulting morphing shape but will also affect how the compliant mechanism transfers the actuation force to the stringer where it is attached.

In this chapter, wingtips containing compliant mechanisms will be subjected to two different morphing load cases (LC1 and LC2) in order to analyze the influence of the mechanism on the morphing shape (comparing to results obtained in the previous chapter) and in order to analyze the effects of the 3D geometrical parameters on the mechanism.

For the purpose of this analysis, it is not necessary to consider the same range of different wingtips as in the previous chapter since the effects of sweep and tapering on the morphing shape have already been discussed and now the inclusion of the mechanism serves to validate the simplification made in SMA and to investigate the change in displacement behavior of the compliant mechanism in a wingtip similar to the one given by Embraer. Thus the following five wingtips will be analyzed in this chapter:

- 0° sweep angle, 0.5 X-taper ratio and 1.0 Y-taper ratio (1500_0_50_100);
- 0° sweep angle, 1.0 X-taper ratio and 0.5 Y-taper ratio (1500_0_100_50);
- 0° sweep angle, 0.5 X-taper ratio and 0.5 Y-taper ratio (1500_0_50_50);
- 35° sweep angle, 1.0 X-taper ratio and 1.0 Y-taper ratio (1500_35_100_100);
- 35° sweep angle, 0.5 X-taper ratio and 0.5 Y-taper ratio (1500_35_50_50);

The code in brackets after every wingtip listed above is used in future plots and tables in order to identify which wingtip is the data referring to. The first number is the span length of the wingtip in mm, the second number is the sweep angle, the third and fourth numbers are the X and Y taper ratio respectively in percentage units.

Each wingtip was subjected to both load cases (LC1 and LC2) and data regarding node displacement of the wingtip skin and of the mechanism is analyzed.

4.1. Results Discussion

Profile Node Results

Table 5 shows the variation of the percentile 90 of the profile node displacement errors when the compliant mechanism is introduced in the model. Considering the wingtips with the presence of only one of the three 3D geometrical parameters (1500_0_50_100, 1500_0_100_50 and 1500_35_100_100), the first noticeable difference is that for the Y-tapered wingtip the percentile 90 values decrease when the mechanisms are introduced

while for the X-tapered and swept wingtips the percentile 90 values increase, meaning that in the analysis made in the previous chapter, the simplification made of not including the mechanisms overestimates the errors for Y-tapering but underestimates the errors for X-tapering and sweep angle.

With this, the important question rises of if the simplification made in the previous chapter invalidates the results obtained. Looking at Table 5, for the first three wingtips, two groups of variations can be made: small variations (considered as less than 5%) and large variations (considered as larger than 30%). Considering the presence of the large variations, it would be sensible to assume that the absence of the mechanisms is not a feasible simplification but with a more detailed view (considering also the absolute values of the percentiles) one can see how the large variations occur when the value of the percentile 90 is small to begin with (lower than 15%) and as the percentile 90 values are larger, the variation of going from LC0 to LC1 becomes smaller.

In conclusion, the simplification made in the previous chapter is valid with the limitation that for profiles with small displacement errors it is much less precise than for profiles with large displacement errors. In other words the results obtained without the mechanisms give a valid description of the order of magnitude of the errors which is in line with the purpose of investigating the effects of 3D geometrical parameters on the morphing shape of the wingtip.

	P2		**P4**	
Wingtip	x	y	x	y
1500_0_50_100	113.75	71.43	0.99	0.88
1500_0_100_50	-4.17	-3.05	-40.60	-48.62
1500_35_100_100	62.03	57.40	43.42	29.79
1500_0_50_50	-38.37	-37.50	-68.72	-66.62
1500_35_50_50	7.84	16.91	-3.26	-3.11

Table 5: Variation [%] in the Percentile 90 values of the profile node displacement error when the compliant mechanisms are introduced (from LC0 to LC1)

Considering the X and Y-tapered wingtip (1500_0_50_50), it can be seen that for low percentile 90 values, their variation when introducing the mechanisms is relatively high (larger than 37%) confirming what was stated above. Also, it is noticeable how there was a decrease in the percentile 90, meaning that the presence of both types of tapering leads to an overestimation of the errors obtained when the mechanism is not present.

Relative to the wingtip containing all three geometrical parameters it is interesting to note how the percentile 90 values are low and yet their variation when going from LC0 to LC1 is also relatively low, leading to the conclusion that the presence of the mechanisms has little effect on the morphing shape when X-taper, Y-taper and sweep angle are present, at least for this specific case (0.5 X and Y taper, 35° sweep angle). Also noticeable is how in P2 the percentile 90 values increase while in P4 they decrease. In all other wingtips the percentile 90 variation has the same direction for both profiles.

Compliant Mechanism Results

From the results obtained it is clear that the introduction of 3D geometrical parameters will alter the compliance behavior of the mechanism by increasing the magnitude of the off-plane displacements. It is noticeable how X-tapering and sweep angle deviate the SR of the mechanism towards the inboard while Y-tapering deviates it towards the outboard.

When X and Y-tapering are combined, the SR deviates towards the outboard having a similar off-plane behavior to when only Y-tapering is present. When sweep angle is also added, the mechanism displays an off-plane displacement distribution similar to when only sweep is present.

Furthermore, with tapering, the bottom part of SB deviates more than SR creating a "*belly*" region in the mechanism while with sweep angle the off-plane displacements continuously increase going from the bottom part of SB to SR. Again when all three geometrical parameters are present the distribution becomes similar to when only sweep is present.

This leads to the conclusion that sweep angle is the leading parameter to determine the mechanism's general off-plane shape. However the presence of tapering decreases the magnitude of the displacements compared to when only sweep is present.

	M2		**M4**	
Wingtip	x	y	x	y
1500_0_50_100	25.5	9.3	-33.7	-64.0
1500_0_100_50	-28.8	-40.0	-28.1	-42.0
1500_35_100_100	-36.4	-24.1	-35.1	-24.4
1500_0_50_50	24.2	44.1	-10.0	-18.4
1500_35_50_50	-23.6	-8.9	-43.8	-46.2

Table 6: Variation [%] between the ideal and the actual target displacements

Relative to the effects on the mechanism output, Table 6 displays the change in the in-plane displacements of the nodes located where the mechanism is designed to displace with a specified value for the different considered wingtips.

As stated before, sweep angle and Y-tapering result in almost identical variations of the target displacements between M2 and M4 suggesting a non

dependence on the location of the mechanism along the span (which does not happen with X-tapering).

When all parameters are put together in the same wingtip, the variations are different between M2 and M4 suggesting that the dependence on mechanism location along the span, shown with X-tapering, is the dominant factor. Thus design corrections made will be different for M2 and M4. Finally the combination of all three parameters result in a decrease of the target displacements for both mechanisms.

5. Conclusions

5.1. Achievements

The main purpose of this thesis was to investigate how 3D geometric parameters (tapering and sweep) would affect the morphing design of the AMWT being done, as part of the EU FP7 project NOVEMOR, since the traditional tools available do not take into account those geometric parameters. To accomplish this a methodology was developed in order to be able to compare wingtips with different geometrical parameters and define an ideal morphing behavior. Furthermore, the methodology was applied in order to obtain data relevant to the AMWT design process being developed.

The first analysis made (SMA) allowed to determine tendencies in the shape morphing behavior of a wingtip (similar to the one being developed) when 3D geometrical parameters are introduced. This data is useful in the wingtip skin design stage where it is necessary to obtain a skin thickness distribution (and skin material properties distribution) that permits morphing to obtain the target shape.

The second analysis (CMA) determined the effects on the mechanism's compliance behavior (without having to go through all of the mechanism's design phases) which is of importance in order to correct or adapt the topology optimization of the mechanism stage. Furthermore this analysis served to validate the simplification made in SMA where the compliant mechanisms are replaced by applying only their desired displacement output to the stringer where they would be connected.

The following section summarizes the conclusions obtained from both analysis.

5.2. Analysis Conclusions

SMA

In terms of displacement errors it was found that, out of the 3 considered parameters, Y-tapering affects the target morphing shape the most leading to larger displacement errors.

Also, it was found that for the same wingtip, the profile with the largest aspect ratio (between P2 and P4) will contain larger displacement errors. When the profile aspect ratio is maintained constant for a wingtip, the profile with the largest errors will be the inboard profile (P4). These two trends are valid for both cases of scaled and not scaled applied displacements.

In terms of the input given to achieve morphing, it was found that the magnitude of the Y component of the applied displacements is strongly correlated to the resulting displacement errors where increasing the applied Y displacements increases the errors. The difference between droop angle of P2 and P4 was also found to be correlated with the resulting displacement errors in the same way although to a lesser extent meaning that if both factors grow in different directions, the overall displacement error change will be according to the change in magnitude of the Y component of the displacement.

For a given profile, it was found that the errors start to increase significantly after the stringer meaning that its position will influence the overall morphing shape error and that the top section of the profile is the most influenced by tapering.

With tapering present, it was found that the introduction of a sweep angle can actually decrease the resulting displacement errors, which is a positive sign since in general wingtips will contain combinations of all 3 considered parameters.

Finally, the introduction of any of the 3D parameters will increase the undesired z component of the displacement.

In terms of stress and strain, it was found that introducing a 3D geometrical parameter will invariably increase the maximum strain and stress. However combining both types of tapering results in a more uniform stress distribution, where the only peak regions are located where the displacements are applied.

In terms of reaction forces, it was found they will solely depend on the geometrical configuration imposed by the changing 3D parameter. For the case of X-tapering and sweep angle, the change in geometrical configuration will result in an increase in the reaction force, while for Y-tapering, the geometrical configuration change can actually result in lower values for the reaction forces.

CMA

The simplification, made in SMA, of substituting the compliant mechanism by applying displacements where it would be attached, was found to be a valid solution in order to enable the analysis of the morphing shape of a larger scope of different wingtips with comparable load cases. With the reserve that when the profile displacement errors are small, the results obtained are less precise.

Relative to the effects on the mechanism, sweep angle was found to be the most determinant 3D

geometrical parameter on the resulting off-plane displacement behavior. Although tapering will influence the magnitude of those displacements and curiously, with all three parameters present in a wingtip, the magnitude of the displacements are smaller than in the wingtip with only sweep.

Finally, relative to the output variation of the mechanisms, it was found that the introduction of 3D parameters will generally decrease the target displacements with the exception of M2 in wingtips 1500_0_50_50 and 1500_0_50_100 (where there is an increase in the target displacement), but since the AMWT contains all three parameters it would be expected that a traditionally designed compliant mechanism will require a larger actuation force in order to obtain the same target displacement. Also, depending on the position of the mechanism along the span (M2 or M4) the change in the desired output will be different.

5.3. Recommendations for Future Work

In order to simplify and speed up the methodology developed, the different tools built should be integrated in order to create a single automatized analysis tool. Furthermore, more parameters can be added to the wingtip CAD model to enable different geometries of the base profile so it can be applied to a bigger variety of wingtips.

The position of the mechanisms along the span and their orientation (in the analysis made in this thesis, the mechanism were positioned always in the xy plane at 1/4 and 3/4 of the span) are variables that can be taken into account and changed in order to optimize the compliant mechanism's morphing capacity.

The stringer's position can also be an added variable since as seen in SMA, profile displacement errors start to increase significantly aft the stringer.

Relative to CMA, an analysis on the changes in stress distribution should also be made (this was not done due to time constraints).

References

[1] Albanesi, A. E., Fachinotti, V. D., and Cardona, A. Design of compliant mechanisms that exactly fit a desired shape. *Asociacin Argentina de Mecnica Computacional*, 28:3192–3205, 2009.

[2] Bagad, V. S. *Mechatronics*. Technical Publications Pune, 4th edition revised edition, 2008.

[3] Barbarino, S., Bilgen, O., Ajaj, R. M., Friswel, M. I., and Inmanl, D. J. A review of morphing aircraft. *Journal of Intelligent Material Systems and Structures*, 22:823–877, 2011.

[4] Bendsoe, M. P. and Sigmund, O. Topology optimization: Theory, methods and applications. *Berlin Heidelberg: Springer-Verlag*, 2003.

[5] BYU. Brigham young university - compliant mechanisms research: Intro to compliant mechanisms. URL `http://compliantmechanisms.byu.edu/content/intro-com` (Accessed 2014).

[6] Howel, L. L. *Compliant Mechanisms*. John Wiley & Sons Inc., 2001.

[7] Kintscher, M., Wiedemann, M., Monner, H. P., Heintze, O., and Kuehn, T. Design of a smart leading edge device for low speed wind tunnel tests in the european project sade. *Institute of Composite Structures and Adaptive Systems, German Aerospace Center, DLR, Braunschweig, Germany*, 2011.

[8] Kota, S., Hetrick, J., Li, Z., and Saggere, I. Tailoring unconventional actuators using compliant transmissions: Design methods and applications. *IEEE/ASME Transactions on Mechatronics*, 4:396–408, 1999.

[9] Lu, K.-J. and Kota, S. Design of compliant mechanisms for morphing structural shapes. *Journal of Intelligent Material Systems and Structures*, 14:379–291, 2003.

[10] Moorhause, D., Sanders, B., von Spakovsky, M., and Butt, L. Benefits and design challenges of adaptive structures for morphing aircraft. *Aeronautical Jornal, Royal Aeronautical Socieaty, London*, 110:157–162, 2006.

[11] Reich, G. W. and Sanders, B. Introduction to morphing aircraft research. *Jornal of Aircraft*, 44:1059, 2007.

[12] Spillman, J. The use of variable camber to reduce drag, weight and costs of transport aircrafts. *Aeronautical Jornal*, 96:1–9, 1992.

[13] Vasista, S., Riemenschneider, J., and Monner, H. P. Design and testing of a compliant mechanism-based demostrator for a droopnose morphing device. *SciTech*, 2015. appearing in press.

[14] Weisshaar, T. A. Morphing technologies - new shapes for aircraft design. *RTO-MP-AVT-141, Neuilly-sur-Seine, France*, 2006.